Nanoscale Res Lett (2010) 5:224–230
DOI 10.1007/s11671-009-9469-5

NANO EXPRESS

Preparation and Characterization of a Lecithin Nanoemulsion as a Topical Delivery System

Huafeng Zhou · Yang Yue · Guanlan Liu · Yan Li · Jing Zhang · Qiu Gong · Zemin Yan · Mingxing Duan

Received: 16 July 2009 / Accepted: 14 October 2009 / Published online: 29 October 2009

Abstract Purpose of this study was to establish a lecithin nanoemulsion (LNE) without any synthetic surfactant as a topical delivery vehicle and to evaluate its topical delivery potential by the following factors: particle size, morphology, viscosity, stability, skin hydration and skin penetration. Experimental results demonstrated that an increasing concentration of soybean lecithin and glycerol resulted in a smaller size LNE droplet and increasing viscosity, respectively. The droplet size of optimized LNE, with the glycerol concentration above 75% (w/w), changed from 92 (F10) to 58 nm (F14). Additionally, LNE, incorporated into o/w cream, improved the skin hydration capacity of the cream significantly with about 2.5-fold increase when the concentration of LNE reached 10%. LNE was also demonstrated to improve the penetrability of Nile red (NR) dye into the dermis layer, when an o/w cream, incorporated with NR-loaded LNE, applied on the abdominal skin of rat in vivo. Specifically, the arbitrary unit (ABU) of fluorescence in the dermis layer that had received the cream with a NR-loaded LNE was about 9.9-fold higher than the cream with a NR-loaded general emulsion (GE). These observations suggest that LNE could be used as a promising topical delivery vehicle for lipophilic compounds.

H. Zhou · Y. Yue · G. Liu · Y. Li · J. Zhang · Q. Gong · M. Duan (✉)
State-Key Laboratory of Biomembrane and Membrane, Biotechnology, School of Life Sciences, Tsinghua University, 100084 Beijing, China
e-mail: duanmx@mail.tsinghua.edu.cn

H. Zhou
e-mail: zhfforever@yahoo.com.cn

H. Zhou · Z. Yan
Jiangsu Longliqi Bioscience Co., Ltd., 215555 Suzhou, China

Keywords Lecithin · Nanoemulsion · Fluorescence · Topical delivery system · Skin hydration

Introduction

Topical delivery systems (TDS) have received increased attention during the past few years. TDS could avoid a variety of disadvantages compared with the oral administration including drastic pH changes, deleterious presence of food and enzymes and first-pass effect of the liver. TDS also eschewed injection inconvenience and needle phobia. In addition, TDS were noninvasive and can be self-administered with the minimization of side-effects in the topical drug therapy. However, the paucity of candidates for TDS was presented in the market because few molecules yielded skin permeability coefficients sufficiently high to meet the clinical therapeutic needs, and TDS was even less applicable for large hydrophilic molecules because of their very low skin permeation rates. The continuous stratum corneum (the outer layer of skin) provided a major barricade for drug penetration to the deeper skin layers and was therefore the usual target for attempts to strength topical drug permeation ability [1–5].

Various kinds of vesicular carriers had been suggested as topical delivery vehicles, including liposomes, microemulsions and lipid nanoparticles [6–10]. However, liposome formulations had certain limitations such as drug loading and stability. Microemulsions, which consisted of synthetic surfactant, oil, water and co-surfactant, exhibited a lower drug-loading capacity relative to the high concentration of surfactant, which had been generally acknowledged to induce skin irritation [11, 12]. Recently, due to advantages such as a controlled droplet size, lower concentration of surfactant and the ability to efficiently

solubilize lipophilic drugs, nanoemulsions, which were composed of nanoscale droplets of one immiscible liquid dispersed within another, had been widely designed to deliver drugs by various routes of administration (e.g., intravenous, oral or ocular delivery) for therapeutic needs [13–17]. Few studies reported nanoemulsions were used as a topical carrier with following significant advantages including powerful penetrability and a high drug-loading capacity [18–21]. Most of nanoemulsions consisted of synthetic surfactant, and nanoemulsions without any synthetic surfactant were rarely reported.

In the present study, we report a LNE system without any synthetic surfactant composed of snake oil [22], soybean lecithin, glycerol and water. The effects of the glycerol to water ratio and soybean lecithin concentration on the emulsion's physical properties (droplet size, viscosity, morphology and stability) were studied. Furthermore, the skin penetration ability and skin hydration levels of this LNE system were determined to evaluate its topical delivery potential.

Materials and Methods

Materials

Soybean lecithin was purchased from Cargill Texturizing Solutions Deutschland GmbH & Co. KG., USA. Refined snake oil and o/w cream were obtained from Jiangsu Longliqi Bioscience Co., Ltd., China. Nile red (NR) was obtained from Sigma–Aldrich, USA. 2-Propanol and optimal cutting temperature compound (OCT) were purchased from Leica microsystem, German. Glycerol, ethane and hexane were reagent grade.

Preparation of LNE

The LNE was composed of 15% (w/w) snake oil, soybean lecithin at varying concentrations of 2.5, 5 and 7.5% (w/w) and an aqueous glycerol solution with glycerol concentrations of 0, 25, 50, 75 and 100% (w/w) as shown in Table 1. Soybean lecithin was dissolved into the snake oil at 50 °C. The oil phase was then stirred in the glycerol aqueous solution at 350 rpm and 50 °C for about 10 min. The mixture was emulsified by stirrer at 1,200 rpm for 2 min. Subsequently, the pre-emulsion obtained was passed through a high pressure homogenizer (NS1001L, Niro Soavi, Italy) at a pressure of 1,000 bar for 4 cycles. Afterward, the hot LNE was cooled to room temperature. Samples were stored at 25 °C for 180 days. To study their stability, samples were stored in a sealed glass bottle at 25 °C and were evaluated in terms of droplet size at fixed times during the first day, 90 and 180 days after the production day.

Table 1 Composition of LNE formulation

Formulation	Ingredients concentration (%,w/w)			
	Snake oil	Soybean lecithin	Glycerol	Water
F1	15	2.5	0	82.5
F2	15	5	0	80
F3	15	7.5	0	77.5
F4	15	2.5	20.6	61.9
F5	15	5	20	60
F6	15	7.5	19.4	58.1
F7	15	2.5	41.25	41.25
F8	15	5	40	40
F9	15	7.5	38.75	38.75
F10	15	2.5	61.9	20.6
F11	15	5	60	20
F12	15	7.5	58.1	19.4
F13	15	2.5	82.5	0
F14	15	5	80	0
F15	15	7.5	77.5	0

Droplet Size and Polydispersity Index (PI)

Droplet size and the PI of LNE were measured by photon correlation spectroscopy (PCS; Zetasize 2000, Malvern Instruments, UK). The LNE was diluted with deionized water by 50-fold. Droplet size and PI value were obtained as the average of three measurements at 25 °C.

Viscosity Measurement

The viscosity of the LNE was measured using the small sample adapter of a Brookfield rheometer (Model DV-III, Brookfield Engineering Labs., Inc., Stoughton, MA, USA) at 25 °C. An average of three data points was obtained to determine the viscosity at a shear rate of 7.34 s^{-1}.

Morphology Measurement

Morphology of the LNE was characterized by freeze-fracture transmission electron microscopy (FF-TEM). Samples were immersed rapidly into liquid ethane cooled by liquid nitrogen. They were then transferred into liquid nitrogen after about 5 s. The samples, after being transferred into the chamber of the freeze-etching apparatus (BALZERS BAF-400D), were fractured at −120 °C and 3×10^{-7} mbar. After being etched for 1 min, Pt–C was sprayed onto the fracture face at 45°, and then C was sprayed at 90°. The replicas were taken out of the chamber and placed on a copper grid mesh after washing with hexane. After processing, morphology data from the samples were detected under a transmission electron microscope (PHILIPS-FEI TECNAI20).

Skin Hydration Test

The skin hydration effect of LNE was investigated in a blind, placebo-controlled in vivo study. LNE was stirred into o/w cream at 200 rpm evenly at 40 °C. Sample 1 was o/w cream without LNE and samples 2, 3, 4 and 5 were o/w cream enriched with 0.5, 2, 5 and 10% LNE (F12, shown in Table 1), respectively. Fifteen volunteers applied the samples on their healthy volar forearm skin. The skin hydration test was conducted at 20 ± 2 °C room temperature and 50 ± 5% relative humidity. Samples were spread on a 3.14 cm^2 area of volar forearm skin with an amount equaling 1.5 μL/cm^2. After application, skin hydration was measured at fixed time intervals of 30, 60, 90, 120 and 150 min with a Corneometer CM 825(CK Electronic GmH, Germany). The percent change in skin hydration was calculated with the following equation: $\Delta\% = (Q_t - Q_0)/Q_0 \times 100$. Q_t was the hydration value after application time t, and Q_0 was the hydration value before application.

Skin Penetration Test

Experiments were conducted on female Wistar SD rats (180–200 g body weight). The rats were 10 weeks old and were of a similar development stage. They were anesthetized by a suitable dose of sodium barbital. The fur on the abdominal area of the rats was carefully removed by an electrical shaver to avoid damage to their stratum corneum. The furless abdominal area was used for in vivo permeation studies.

In this study, NR, a fluorescent dye, was dissolved into the oil phase during the LNE preparation procedure. The following two samples were used in a blind, placebo-controlled in vivo study: one sample was the o/w cream incorporated with NR-loaded LNE (F12, shown in Table 1); the other was the o/w cream incorporated with NR-loaded GE (F12 without HPH). The NR concentration in the o/w cream was 2.5 μg/mL, and the NR-loaded GE or NR-loaded LNE were stirred into the o/w cream at 200 rpm evenly at 40 °C. For each set of experiments, 50 mg of sample was applied to the hairless abdominal skin area of ~3.14 cm^2. At fixed times of 0.5, 2 and 4 h after application, the surplus sample was removed from the skin surface, the skin surface was washed three times with PBS and dried gently under cold air with an electric hair-drier. A 0.5 cm × 0.5-cm skin piece, which was cut out from the treated area, was embedded in optimal cutting temperature compound and frozen rapidly by liquid nitrogen. The specimen was removed from liquid nitrogen and was frozen on a metal block. The metal block was then transferred to a cryostat microtome (LE ICACM 1850, Germany) for slicing through vertical cross-sections of skin. Twelve vertical skin sections with a thickness of 25 μm were obtained and stored at 4 °C until analyzed microscopically.

Skin sections were subjected to fluorescent microscopy using an Olympus CK40 microscope (Olympus, Japan) equipped with a UV source and filter for fluorescent measurements. Image capture and analysis were carried out by the Image-pro Plus program (Media Cybernetics, USA). The excitation and emission wavelengths were 543 nm and 604 nm for NR, respectively. Images were recorded with a camera integration time of 1/1.8 s, and the same parameters were used for the imaging of all samples. The fluorescence intensity value was quantified using Image-pro Plus program.

Data Analysis

All the data tests were repeated three times and expressed as the mean ± SD. The statistical data were analyzed by a t-test analysis via Origin 7.0.

Results and Discussion

Particle Size and Viscosity of LNE

The mean droplet size of F1-F9 was in the range of 310–100 nm with a PI value ranging from 0.6 to 0.2, while the mean droplet size of F10-F15 was in the range of 100–50 nm with a PI value from 0.2 to 0.1 (shown in Table 2).

Table 2 Droplet size, polydispersity index (PI) and viscosity of LNE (mean ± SD, $n = 3$)

Formulation	Droplet size (nm)	PI	Viscosity (mPa.s)
F1	309 ± 11	0.58 ± 0.09	2.3 ± 0.1
F2	282 ± 9	0.43 ± 0.06	5.2 ± 0.4
F3	240 ± 4	0.32 ± 0.05	12.1 ± 0.3
F4	238 ± 6	0.28 ± 0.04	11.6 ± 0.7
F5	212 ± 4	0.26 ± 0.03	15.2 ± 0.5
F6	182 ± 5	0.24 ± 0.03	32.3 ± 1.9
F7	163 ± 4	0.23 ± 0.04	24.1 ± 1.6
F8	145 ± 2	0.25 ± 0.03	43.6 ± 0.8
F9	113 ± 3	0.21 ± 0.02	71.2 ± 2.1
F10	92 ± 4	0.17 ± 0.03	68.4 ± 3.2
F11	79 ± 2	0.15 ± 0.04	83.2 ± 1.9
F12	68 ± 2	0.13 ± 0.02	136.7 ± 5.2
F13	71 ± 3	0.11 ± 0.01	565.7 ± 13.1
F14	58 ± 2	0.09 ± 0.03	989.6 ± 15.2
F15	75 ± 4	0.12 ± 0.05	1,574.8 ± 12.5
F12 (without HPH)	1,742 ± 102	1.34 ± 0.21	375.2 ± 4.7

An increase in soybean lecithin concentration from 2.5 to 7.5% (w/w) resulted in a decrease in particle size (mean droplet size of F1-F3 were from 309 to 240 nm, mean droplet size of F4-F5 were from 238 to 182 nm, mean droplet size of F7-F9 were from 163 to 113 nm and the mean droplet size of F10-F12 were from 92 to 68 nm) at an increasing glycerol concentration except at glycerol concentration of 100% (w/w), which pronounced an increase in droplet size (from 58 to 75 nm) at a lecithin concentration of 7.5% (w/w). The viscosity of LNE was shown in Table 2, and the viscosity of LNE increased with the increase in glycerol concentration and lecithin content. When the glycerol concentration was less than 75%, the viscosity was below 200 mPa s. However, when the glycerol concentration was 100%, the viscosity significantly increased, and the maximum viscosity reached 1,574.8 mPa s (F15). A possible explanation of the droplet size reduction after an increased soybean lecithin concentration and an increased glycerol content is that soybean lecithin freely moved and was able to absorb around the snake oil droplet, thereby resulting in an increased surface to volume ratio of the droplet. Moreover, soybean lecithin, localized to the surface of the emulsion particles, reduced interfacial free energy and provided a mechanical barrier to coalescence [23], while glycerol in the continuous aqueous phase reduced the water's surface tension. At a glycerol concentration of 100%, an increased soybean lecithin concentration resulted in a sharp increase in the viscosity of the continuous aqueous phase, especially at a soybean lecithin concentration of 7.5%. This high viscosity generated difficulty in lecithin movement and a rapid covering of the oil droplet during the preparation procedure to prevent any coalescence.

Interestingly, apart from the size and viscosity, the effect of glycerol on the emulsion appearance was also observed. When the formulation was composed of 0 and 25% (w/w) glycerol in the aqueous phase (F1-F6), the nanoemulsion appeared as a milky solution. When the formulation was composed of 50% glycerol in the aqueous phase (F7-F9), the nanoemulsion appeared as a semitransparent solution. Furthermore, when the glycerol concentration was increased to 75 and 100% in the aqueous phase (F10-F15), the nanoemulsion appeared as a transparent solution. Possibly, glycerol behaved as a continuous phase solvent, whereby it not only affected the appearance of the nanoemulsion but also increased the viscosity of the continuous phase so as to decrease the droplet collision frequency [24, 25].

Morphology of LNE

FF-TEM has emerged as an artifact-free method for observing diverse systems such as surfactant aggregates, polymer and polymer–surfactant solutions, and microemulsions, as well as biological and biomedical systems. These methods provide the ability to observe microstructures by rapid vitrification of the solution containing the aggregates [26–28]. The morphology of the LNE was observed with FF-TEM, but only micrographs of

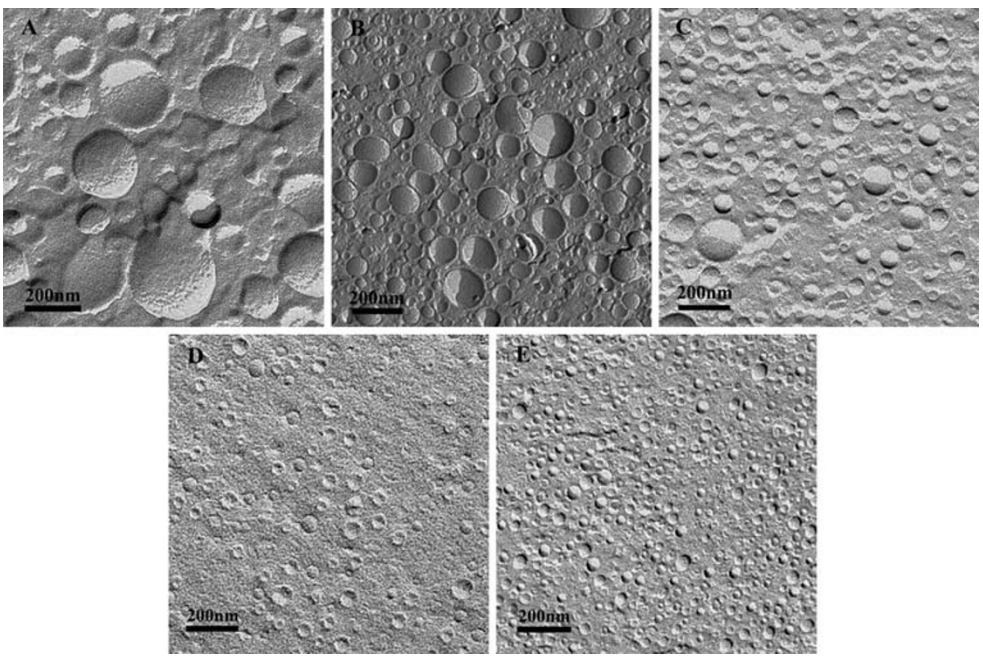

Fig. 1 TEM micrograph of different LNEs. The images represent the LNE F2 (**a**), the LNE F5 (**b**), the LNE F8 (**c**), the LNE F11 (**d**) and the LNE F14 (**e**)

formulations of F2, F5, F8, F11 and F14 are shown in Fig. 2. From all of the five images, only the formulation with no glycerol (Fig. 1a) exhibited an irregular spherical shape, and the distribution of the droplet size was uneven with a large PI value (0.43), as confirmed by the PCS. Furthermore, agglomeration of the droplet was present in Fig. 1a. When 25% glycerol was added to the aqueous phase, the sphere shape of the nanoemulsion became more regular and smaller droplets were dominant (Fig. 1b). When the concentration of glycerol increased sequentially, the formulation exhibited a standard spherical shape, and the distribution of droplet size became more homogenous. In Fig. 1e, the droplet was in a standard spherical shape in pure glycerol, and the distribution of droplet size was very homogenous, as certificated by the PCS with a 0.09 PI value. Form the above discussion, all the formulations were in a spherical shape, and the extent was affected by the glycerol concentration. As the concentration of glycerol increased, the morphology of the LNE was more spherical and the monodispersity of the LNE droplets was improved.

Stability of LNE

Droplet size was used as a stability index for all formulations stored at 25 °C for 180 days (Fig. 2). Most of the formulations revealed an increase in droplet size with the increasing concentration of glycerol. However, the size change became undistinguishable when the concentration of glycerol reached 100%. The formulation (F1–F5) mean droplet size was significantly increased after 90 and 180 days of storage. Oswald ripening, the growth in the size of droplets as the contents of one drop diffuses into another, primarily affects nanoemulsions and is the most serious instability concern for nanoemulsions. If there is any diffusion of the contents of the dispersed phase, large droplets grow larger at the expense of smaller droplets, and the average size of the droplet distribution will continually increase. For an o/w nanoemulsion, the rate of ripening is directly related to the water solubility of the oil. In an ideal situation with a perfectly monodispersed distribution, there should be no ripening due to the lack of differences in the solubility of droplets based on size. Thus, narrow distributions will be more resistant to Oswald ripening than broader distributions [21, 29, 30].

Skin Hydration of LNE

The results of the skin hydration assay are shown in Fig. 3. After application, all the formulations increased the skin hydration level. However, the formulation that contained LNE improved the hydration more significantly than the formulation without LNE, and changes in hydration levels increased with the increasing concentration of LNE from 0.5 to 10%. After 150 min, changes in skin hydration were 24.5, 31.9, 39.3, 43.6 and 72.8% for formulations A, B, C, D and E, respectively. One explanation for these effects is that maybe nanoemulsion droplets adhere to the skin and form a dense film that inhibits water evaporation from the skin. Notably, nanoemulsions exhibit distinct adhesive properties to skin surfaces. Hence, as the water evaporated from the nanoemulsion dispersion area, a film formed of nanoemulsion droplets stayed on the skin. The capillary forces of the nanometer pores between the nanoemulsion droplets are contractive and promote fusion and dense film formation, which is also promoted by the application of pressure [8, 31]. The absorption of some topically applied drugs and cosmetics may be improved due to increased skin hydration [32, 33].

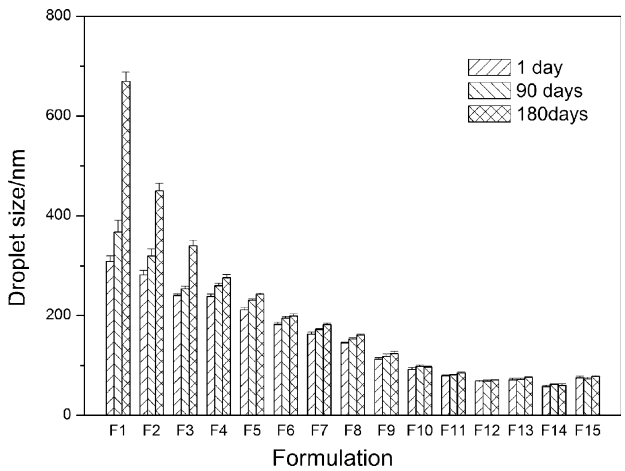

Fig. 2 Stability of LNE size during storage at 25 °C (mean ± SD, $n = 3$)

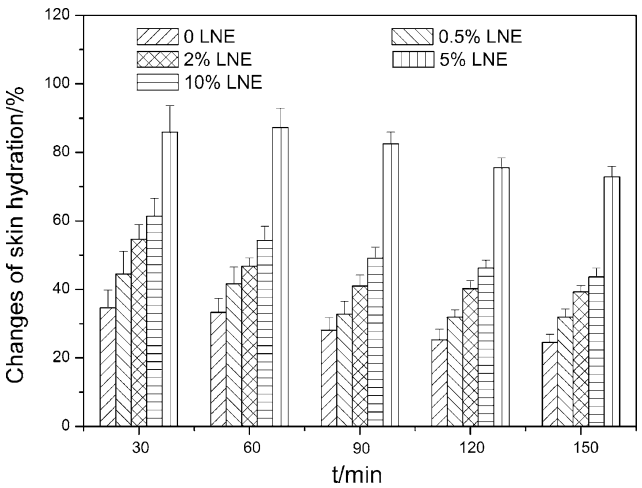

Fig. 3 Effect of LNE on changes in skin hydration after incorporated into o/w cream (mean ± SD, $n = 3$)

Skin Penetration of LNE

Images of skin without applying any fluorescent dye revealed a weak fluorescent signal, which was also contributed to skin autofluorescence. However, the autofluorescence signal was deducted when the photograph of the skin slice (applied with NR dye) was taken. Figure 4a and b depicts representative examples of fluorescence microscopy images of vertically cross-sectioned skin following topical application of the above two formulations for 0.5, 2 and 4 h. Significantly, LNE with droplet sizes of about 68 nm clearly promoted penetration of NR into the deeper layers of skin when compared to a GE with a droplet size of about 1,742 nm. The intensity of the NR dye increased with time until 4 h. Quantitative analysis of the dye penetration was obtained from pixel intensities derived from fluorescence measurements of skin slices. The dermis skin fluorescence measurement of NR was expressed in arbitrary unit (ABU) and is shown in Fig. 4c. A significant difference ($p < 0.01$) was detected in all the skin dermal layers between the above two formulations. At fixation times of 0.5, 2 and 4 h, the ABU value of fluorescence in the dermis layer that had received the formulation with LNE was 3.7-, 7.3- and 9.9-fold higher than the respective one with GE. The significant extent of the skin penetration of the LNE formulation was most likely attributed to the fact that nanoemulsions provide superior skin hydration, which has been shown to be helpful for improving permeation effects [34]. Assuming that the average width of the transepidermal hydrophilic pathway is up to ~100 nm, which is similar to the intercorneocyte space, it is conceivable that nanosized droplets are able to traverse through the interconeocyte spaces [35, 36]. An increase in the extent of penetration may result from an alteration in the barrier properties and a greater degree of partitioning of the lecithin nanoemulsion into the stratum corneum [37]. In future studies, the mechanisms of lecithin nanoemulsion penetration, cellular uptake, potential toxicity in skin cells and the topical delivery of lipophilic drugs should be investigated.

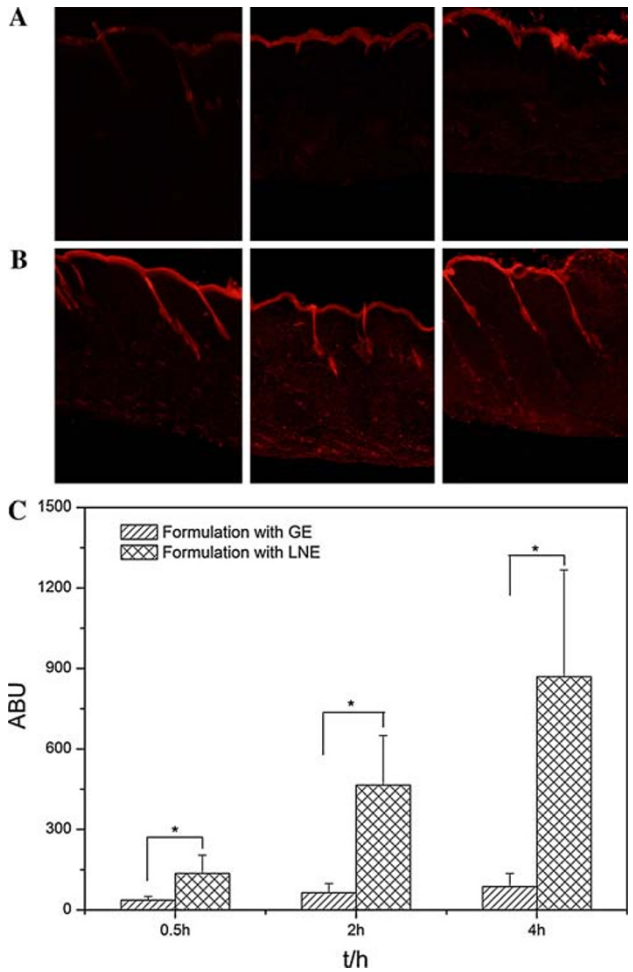

Fig. 4 Fluorescent images of skin slices and fluorescent ABU values of the dermis layer at the fixed times of 0.5, 2 and 4 h after the application of the formulation with (2.5 μg/mL) NR dye. **a** Fluorescent images of skin slices applied with a formulation of GE; **b** fluorescent images of skin slices applied with formulations of LNE and **c** distribution of fluorescent ABU values in the dermis layer (* $p < 0.01$, mean ± SD, $n = 3$)

Conclusions

The LNE, composed of snake oil, soybean lecithin, glycerol and water, was prepared by a HPH method successfully. Results revealed that LNE not only improved the skin hydration of formulation significantly, but also greatly strengthened skin penetration of NR for topical application. LNE may be a promising topical delivery vehicle for lipophilic compounds.

Acknowledgments The authors are grateful for FF-TEM support by Shufeng Sun from the Center for Electron Microscope, Institute of Biophysics, Chinese Academy of Sciences, China.

References

1. A.C. Williams, B.W. Barry, Adv. Drug Deliv. Rev. **56**, 603 (2004). doi:10.1016/j.addr.2003.10.025
2. M.R. Prausnitz, R. Langer, Nat. Biotechnol. **26**, 1261 (2008). doi:10.1038/nbt.1504
3. H.F. Zhou, Q.H. Ma, Q. Xia, N. Gu, Solid State Phenom. **121–123**, 271 (2007)
4. M.J. Lawrence, G.D. Rees, Adv. Drug Deliver. Rev. **45**, 89 (2000). doi:10.1016/S0169-409X(00)00103-4
5. M. Changez, M. Varshney, Drug Dev. Ind. Pharm. **26**, 507 (2000). doi:10.1081/DDC-100101261
6. H. Rosen, T. Abribat, Nat. Rev. Drug Discov. **4**, 381 (2005). doi:10.1038/nrd1721
7. M. Kreilgaard, E.J. Pedersen, J.W. Jaroszewski, J. Control. Release **69**, 421 (2000). doi:10.1016/S0168-3659(00)00325-4

8. R.H. Müller, M. Radtke, S.A. Wissing, Adv. Drug Deliv. Rev. **54**(Suppl. 1), S131 (2002). doi:10.1016/S0169-409X(02)00118-7
9. Y.Y. Lu, H.F. Zhou, Q. Xia, Q.H. Ma, N. Gu, Chin. J. Pharm. **37**, 17 (2006)
10. H.F. Zhou, Q.H. Ma, Y. Ding, Q. Xia, N. Gu, Chin. J. Process Eng. **6**, 598 (2006)
11. M. Kreilgaard, Adv. Drug Deliv. Rev. **54**(Suppl. 1), S77 (2002). doi:10.1016/S0169-409X(02)00116-3
12. R. Bajoria, S.R. Sooranna, Placenta **19**, 265 (1998). doi:10.1016/S0143-4004(98)80048-9
13. N.S. Santos-Magalhaes, A. Pontes, V.M.W. Pereira, M.N.P. Caetano, Int. J. Pharm. **208**, 71 (2000). doi:10.1016/S0378-5173(00)00546-9
14. G. Nicolaos, S. Crauste-Manciet, R. Farinotti, D. Brossard, Int. J. Pharm. **263**, 165 (2003). doi:10.1016/S0378-5173(03)00365-X
15. S. Tamilvanan, S. Schmitd, R.H. Muller, S. Benita, Eur. J. Pharm. Biopharm. **59**, 1 (2005). doi:10.1016/j.ejpb.2004.07.001
16. E. Yilmaz, H.H. Borchert, Int. J. Pharm. **307**, 232 (2006). doi:10.1016/j.ijpharm.2005.10.002
17. M. Bivas-Benita, M. Oudshoorn, S. Romeijn, K. Meijgaarden, J. Control. Release **100**, 145 (2004). doi:10.1016/j.jconrel.2004.08.008
18. M.P. Piemi, D. Korner, S. Benita, J.P. Marty, J. Control. Release **58**, 177 (1999). doi:10.1016/S0168-3659(98)00156-4
19. C. Solans, P. Izquierdo, J. Nolla, N. Azemar, M.J. Garcia-Celma, Curr. Opin. Colloid Interface Sci. **10**, 102 (2005). doi:10.1016/j.cocis.2005.06.004
20. O. Sonneville-Aubrun, J.T. Simonnet, F. L'Alloret, Adv. Colloid Interface Sci. **108–109**, 145 (2004). doi:10.1016/j.cis.2003.10.026
21. T. Tadros, P. Izquierdo, J. Esquena, C. Solans, Adv. Colloid Interface Sci. **108–109**, 303 (2004). doi:10.1016/j.cis.2003.10.023
22. N. Shirai, H. Suzuki, R. Shimizu. Fisheries Sci. **68**, 239 (2002). doi:10.1046/j.1444-2906.2002.00417.x
23. H. Reiss, J. Colloid Interface Sci. **53**, 61 (1975). doi:10.1016/0021-9797(75)90035-1
24. W. Chanasattru, I.A. Decker, D.J. McClements, Food Hydrocolloid **23**, 253 (2009). doi:10.1016/j.foodhyd.2008.02.004
25. S. Usawadee, N. Onanong, U. Napaporn, Int. J. Pharm. **372**, 105 (2009). doi:10.1016/j.ijpharm.2008.12.029
26. M. Brandl, M. Drechsler, D. Bachmann, K. Bauer, Chem. Phys. Lipids **87**, 65 (1997). doi:10.1016/S0009-3084(97)00028-5
27. T. GulikKrzywicki, Curr. Opin. Colloid Interface. Sci. **2**, 137 (1997)
28. Y.L. Yan, N.S. Zhang, C.T. Qu, L. Liu, Colloids Surf. A **264**, 139 (2005). doi:10.1016/j.colsurfa.2005.04.025
29. P. Taylor, Adv. Colloid Interface Sci. **75**, 107 (1998). doi:10.1016/S0001-8686(98)00035-9
30. P. Taylor, Adv. Colloid Interface Sci. **106**, 261 (2003). doi:10.1016/S0001-8686(03)00113-1
31. S.A. Wissing, PhD Thesis, Free University Berlin, 2002
32. S. Diane, W.B. Brian, Int. J. Pharm. **22**, 291 (1984). doi:10.1016/0378-5173(84)90029-2
33. C. Gregor, G. Dieter, Biophysical J. **84**, 1010 (2003). doi:10.1016/S0006-3495(03)74917-0
34. H.B. Gunt, G.B. Kasting, Eur. J. Pharm. Sci. **32**, 254 (2007). doi:10.1016/j.ejps.2007.07.009
35. B.W. Barry, Eur. J. Pharm. Sci. **14**, 101 (2001). doi:10.1016/S0928-0987(01)00167-1
36. G. Cevc, Adv. Drug Deliv. Rev. **56**, 675 (2004). doi:10.1016/j.addr.2003.10.028
37. B.W. Barry, Nat. Biotechnol. **22**, 165 (2004). doi:10.1038/nbt0204-165